https://doi.org/10.5194/hess-2019-332
Preprint. Discussion started: 4 July 2019

Hydrology and Earth System Sciences
Discussions

Improving lake mixing process simulations in the Community Land Model by using K profile parameterization

Qunhui Zhang[1], Jiming Jin[1,2], Xiaochun Wang[3], Phaedra Budy[4,2], Nick Barrett[2], Sarah E. Null[2]

[1]College of Water Resources and Architectural Engineering, Northwest A & F University, Yangling, Shaanxi 712100, China

[2]Department of Watershed Sciences, Utah State University, Logan, Utah 84322, USA

[3]JIFRESSE, University of California, Los Angeles, 90095, USA

[4]US Geological Survey, Utah Cooperative Fish & Wildlife Research Unit, Logan, Utah 84322, USA

Correspondence to: Jiming Jin (jiming.jin@usu.edu)

Abstract. We improved lake mixing process simulations by applying a vertical mixing scheme, K profile parameterization (KPP), in the Community Land Model (CLM) version 4.5, developed by the National Center for Atmospheric Research. Vertical mixing of the lake water column can significantly affect heat transfer and vertical temperature profiles. However, the current vertical mixing scheme in CLM assumes that mixing is driven primarily by wind, and it produces large biases in thermal process simulations. We improved the CLM lake model by using KPP, where vertical mixing was driven by winds and surface thermal forcing, the latter representing the net heat flux in the lake boundary layer. We chose an Arctic Alaskan lake to evaluate this improved lake model. Results demonstrated that KPP could reproduce the observed lake mixing and significantly improved lake temperature simulations when compared to the original mixing scheme in CLM. Our newly improved model better represents the transition between stratification and turnover due to surface thermal forcing combined with high winds. This improved lake model has great potential for reliable physical lake process predictions and better ecosystem services.

1 Introduction

Lake thermal processes are vital to improving our understanding of regional climate systems. Lakes significantly affect regional temperature, precipitation, and surface heat fluxes (Jeffries et al., 1999; Lofgren, 2004; Long et al., 2007; Rouse et al., 2008; Thiery et al., 2015). In fact, lakes can reduce

https://doi.org/10.5194/hess-2019-332
Preprint. Discussion started: 4 July 2019

Hydrology and Earth System Sciences
Discussions
Open Access
EGU

diurnal temperature variation by cooling near-surface air temperature during the day and warming it at night (Bonan, 1995; Krinner, 2003; Samuelsson et al., 2010). Regional climate modeling has shown that lakes can have a strong effect on seasonal precipitation (Diallo et al., 2017; Zhu et al., 2017). For instance, lakes cool the lower atmosphere during the summer and increase its stability, reducing summer precipitation as compared to the land (Gu et al., 2016; Sun et al., 2015). Additionally, large lakes, like the Great Lakes in North America, often produce strong snowstorms during early winter or spring from high surface evaporation (Dai et al., 2018; Laird et al., 2009). Furthermore, Rouse et al. (2005) indicated that lakes affect surface energy balance, with higher net radiation, subsurface heat storage, and evaporation than the nearby land.

Lake temperatures shape lake ecosystems (Marshall et al., 2013; Michalski and Lemmin, 1995). For example, Berger et al. (2006) showed that plankton biomass is negatively correlated with lake mixed layer depth. Some studies have proven that strong temperature stratification stimulates the spring phytoplankton bloom (Chiswell, 2011; Mahadevan et al., 2012). What is more, the frequency and intensity of water turnover, a product of the thermal processes within a lake, is critical for replenishing and circulating hypolimnetic O_2 and nutrients (Dodson, 2004; Foley et al., 2012; Shimoda et al., 2011). Hence, it is important to accurately quantify lake thermal processes in order to fully comprehend how temperatures affect lake ecosystems.

Numerical models are important tools for investigating lake thermal processes. Vertical mixing processes need to be parameterized in these models. The usefulness of these models depends on whether they can represent lake processes accurately and in a dynamic consistent manner. Several one-dimensional (1-D) lake models have been developed over the last three decades with varying levels of sophistication in terms of how model physics and structure are represented (Henderson-Sellers, 1985; Goudsmit et al., 2002; Mironov, 2008; Stepanenko et al., 2016). The Lake Model Inter-comparison Project (LakeMIP) assessed the simulation skill of different models (Stepanenko et al., 2010) and concluded that no single lake model is capable of simulating thermal processes for a wide range of lakes with different depths (Kheyrollah Pour et al., 2012; Stepanenko et al., 2014; Martynov et al., 2010; Perroud et al., 2009; Yao et al., 2014). Stepanenko et al. (2012) indicated that the poor skill in modeling lake thermal processes was due to the simplification of water mixing processes so that they were driven primarily by near-surface wind. Martynov et al. (2010) showed that focusing on wind-driven mixing often leads to insufficient water mixing and thus weakened heat transfer within the

https://doi.org/10.5194/hess-2019-332
Preprint. Discussion started: 4 July 2019

lake, resulting in unrealistic spring warming and fall cooling of the lake surface. Hence, efforts have been made to improve lake mixing simulations through enlarged eddy diffusivity (Gu et al., 2013; Perroud et al., 2009; Xu et al., 2016). However, such an approach mostly strengthens mixing in the entire water body, which often greatly overestimates water mixing in the lower part of lakes (Subin et al., 2012; Zhang et al., 2018).

Based on observational studies, surface thermal forcing plays a vital role in driving lake mixing in addition to wind (MacIntyre et al., 2009). Lake water mixing is affected by not only winds, but air-lake heat exchange and net radiation as well (Chowdhury et al., 2015; Ellis et al., 1991; Imberger, 1985; Lewis, 1973; MacIntyre, 2008; Patterson et al., 1984; Yang et al., 2015). Surface thermal forcing, also called buoyancy flux, is defined as the net heat flux in the boundary layer. A lake gains energy with a positive buoyancy flux and loses energy with a negative buoyancy flux. Studies have shown that negative buoyancy fluxes combined with high winds can break up summer lake stratification (Augusto-Silva et al., 2019; Liu et al., 2019; Saber et al., 2018). Therefore, besides winds, surface thermal forcing (buoyancy flux) is an essential factor that affects lake water mixing.

K profile parameterization (KPP) (Large et al., 1994), an advanced water mixing scheme used mostly in ocean models, makes significant improvements in oceanic water mixing simulations (Li et al., 2001; Roekel et al., 2018; Shchepetkin and Mcwilliams, 2005; Wang et al., 2013). KPP considers the effects of both wind and surface thermal forcing on water mixing. The objective of this study was to improve lake mixing process simulations by using KPP with the Community Land Model (CLM) version 4.5, developed by the National Center for Atmospheric Research (Oleson et al., 2013). This newly improved model was then applied to an Arctic Alaskan lake for model validation. In this paper, Sect. 2 introduces the mixing schemes, data, and methodology, Sect. 3 presents simulation results and analysis, and conclusions are given in Sect. 4.

2 Mixing schemes, data, and methodology

2.1 Mixing scheme descriptions

2.1.1 The original mixing scheme in the CLM lake model

The 1-D lake model embedded in the current CLM version (CLM-ORG) simulates heat and water exchanges between the air and lake surface, water phase changes, and radiation transfer and water

https://doi.org/10.5194/hess-2019-332
Preprint. Discussion started: 4 July 2019

Hydrology and Earth System Sciences
Discussions
Open Access
EGU

mixing within the lake. The lake model consists of up to 5 snow layers on the lake ice, 10 water and ice layers, 10 soil layers, and 5 bedrock layers. Researchers have attempted to advance this lake model to more closely reflect reality over the last two decades (Fang and Stefan, 1996; Henderson-Sellers, 1985; Hostetler and Bartlein, 1990; Subin et al., 2012). The total eddy diffusivity in the lake model is calculated as follows (Subin et al., 2012):

$$K_w^{ORG} = m_d(\kappa_e + K_{ed} + \kappa_m) \quad (1)$$

where κ_e represents wind-driven diffusivity ($m^2\ s^{-1}$), K_{ed} is the enhanced eddy diffusivity for unresolved mixing processes ($m^2\ s^{-1}$), κ_m is a constant molecular diffusivity equal to 1.4×10^{-7} $m^2\ s^{-1}$, and m_d is a parameter to increase the diffusivity for deep lakes, which is equal to 10 when lake depth is greater than 25 m. Wind-driven diffusivity, κ_e, is formulated as follows:

$$\kappa_e = \begin{cases} \frac{\kappa w^* z}{P_0(1+37Ri^2)}\exp(-k^* z), & T_g > T_f \\ 0, & T_g \le T_f \end{cases} \quad (2)$$

where T_g is the water surface temperature (WST) (K), T_f is the freezing temperature, equal to 273.15 K, κ is the von Karman constant, P_0 is the turbulent Prandtl number, equal to 1, z is depth, which increases downward (m), w^* is the surface friction velocity ($m\ s^{-1}$) equal to $0.0012u_2$, where u_2 is the 2 m wind speed ($m\ s^{-1}$), and k^* is related to latitude φ:

$$k^* = 6.6u_2^{-1.84}\sqrt{|\sin\varphi|} \quad (3)$$

Ri is the Richardson number, given as:

$$R_i = \frac{-1+\sqrt{1+\frac{40N^2\kappa^2z^2}{w^{*2}\exp(-2k^*z)}}}{20} \quad (4)$$

where N is the local buoyancy frequency representing the stability of water,

$$N^2 = \frac{g\partial\rho}{\rho\partial z} \quad (5)$$

g is gravity acceleration ($m\ s^{-2}$), and ρ is the density of water ($kg\ m^{-3}$). The equation of the enhanced diffusivity is:

$$K_{ed} = 1.04\times10^{-8}(N^2)^{-0.43}, (N^2 \ge 7.5\times10^{-5}\ s^2) \quad (6)$$

When N^2 is the minimum reaching to about 7.5×10^{-5} s^2, the enhanced diffusivity is about six times more than the molecular diffusivity (Fang and Stefan, 1996). The wind-driven diffusivity is typically at least 2 orders larger than the molecular diffusivity (Hostetler and Bartlein, 1990). Thus, winds have a dominant effect on water mixing in the CLM lake model. In practical application, the total eddy

https://doi.org/10.5194/hess-2019-332
Preprint. Discussion started: 4 July 2019

Hydrology and Earth System Sciences
Discussions

diffusivity computed by Eq. (1) generally produces unrealistically weak mixing and causes large errors in temperature profile simulations (Gu et al., 2013; Zhang et al., 2018).

2.1.2 KPP

KPP has two different eddy diffusivity parameterizations for the lake boundary layer and the layer below, which is different from the eddy diffusivity represented in the original CLM lake model. The diffusivity of the lake boundary layer, a function of wind and surface thermal forcing, is based on the Monin-Obukhov similarity theory (Monin and Obukhov, 1954):

$$K_w^{KPP}(\sigma) = hw(\sigma)G(\sigma) + \kappa_m \quad (7)$$

where $\sigma = d/h$ is the dimensionless vertical coordinate varying from 0 at the lake surface to 1 at the bottom of the lake boundary layer (h), $w(\sigma)$ is the velocity scale, and $G(\sigma)$ is the shape function. κ_m is a constant molecular diffusivity, as in Eq. (1). The velocity scale is:

$$w(\sigma) = \begin{cases} \dfrac{\kappa u^*}{\emptyset\left(\frac{\varepsilon h}{L}\right)}, \varepsilon < \sigma < 1, \zeta < 0 \\ \dfrac{\kappa u^*}{\emptyset(\frac{\sigma h}{L})}, \qquad otherwise \end{cases} \quad (8)$$

where κ is the von Karman constant (0.4), ε is equal to 0.1, u^* is the surface friction velocity, $\phi(\zeta)$ is a non-dimensional flux profile associated with the stability parameter $\zeta = d/L = \sigma h/L$, L is the Monin-Obukhov length scale defined as $L = u^{*3}/\kappa B_f$ and the buoyancy flux $B_f = H^* g\alpha C_p^{-1}\rho^{-1}$. H^* is the sum of the surface turbulent heat fluxes, net long-wave radiation, and net shortwave radiation for the lake boundary layer, α is the constant thermal expansion coefficient, and C_p is the specific heat capacity of water (J kg^{-1} K^{-1}). The non-dimensional shape function $G(\sigma)$ is a third-order polynomial (see the Appendix).

Water mixing below the lake boundary layer considers vertical shear and internal waves. The equation is:

$$K_w^{KPP} = k_s + k_w + \kappa_m \quad (9)$$

where k_s is the diffusivity due to shear instability, and k_w is the internal wave diffusivity set to a constant (10^{-7} m^2 s^{-1}) as the background diffusivity (Bryson and Ragotzkie, 1960; Powell and Jassby, 1974; Thorpe and Jiang, 1998). The shear mixing term is calculated as:

https://doi.org/10.5194/hess-2019-332
Preprint. Discussion started: 4 July 2019

Hydrology and Earth System Sciences
Discussions
Open Access
EGU

$$k_s = \begin{cases} k_0, & Ri_g < 0 \\ k_0\left[1 - (Ri_g/Ri_0)^2\right]^p, & 0 < Ri_g < Ri_0 \\ 0, & Ri_0 < Ri_g \end{cases} \quad (10)$$

where $k_0 = 10^{-5}$ m^2 s^{-1} (Etemad-Shahidi and Imberger, 2006; Saber et al., 2018; Sweers, 1970), $Ri_0 = 0.7$, and $p = 3$. Ri_g is the local gradient Richardson number:

$$Ri_g = \frac{N^2}{\left(\frac{\partial V}{\partial z}\right)^2} \quad (11)$$

$$V = V_{sfc}\left(3\left(\frac{z}{D}\right)^2 - 4\left(\frac{z}{D}\right) + 1\right) \quad (12)$$

$$V_{sfc} = 0.028W \quad (13)$$

where V is the horizontal velocity of water (m/s), D is the lake depth, V_{sfc} is the surface water flow velocity, and W is the surface wind. To apply KPP in the CLM lake model, we use Eq. (12) to represent the change of water flow in the vertical direction over the entire lake depth (D) (Banks, 1975; Jan and Verhagen, 1994). We can see in Eq. (13) that V_{sfc} is linked with W (Stanichny et al., 2016; Wu, 1975).

The boundary layer depth depends mainly on the buoyancy and horizontal water flow velocity profiles. In order to compute the boundary layer depth, the bulk Richardson number is first computed as follows:

$$Ri_b(d) = \frac{\left(B_r - B(d)\right)d}{|V_r - V(d)|^2 + V_t^2(d)} \quad (14)$$

where Ri_b is the bulk Richardson number, and B is the buoyancy. When Ri_b is equal to 0.25 (Kunze et al., 1990; Peters et al., 1995), the shallowest water depth (d) is treated as the depth of the lake boundary layer. The subscript r represents the near-surface water layer with a depth of 0.1 m ($B_r, B(d), V_t^2(d)$, see the Appendix).

In this study, KPP was implemented into the CLM lake model (CLM-KPP) to improve lake mixing process simulations. As with CLM-ORG, the input variables to KPP consist of the lake depth, surface wind, and water density of each layer. In addition, KPP needs the buoyancy flux for the lake boundary layer. Outputs from KPP contain the total eddy diffusivity of each layer and the lake boundary layer.

2.2 Study area

We selected an Arctic Alaskan lake with available data to evaluate the original lake mixing scheme and KPP. Fog 3 Lake is in Arctic Alaska at (68.67˚ N, 149.10˚ W) (Fig. 1). In 2018 it had a surface area of

https://doi.org/10.5194/hess-2019-332
Preprint. Discussion started: 4 July 2019

150 35,230 m^2 and a maximum depth of 19.74 m. The lake has a long ice duration, and ice-off is usually in late June, while ice-on typically occurs in early October (Arp et al., 2015).

2.3 Data

Observed hourly meteorological station data were used to force CLM with the two water mixing schemes: the wind-only driven scheme and KPP. This station is ~1.5 km from Fog 3 Lake, and the
155 forcing variables include downward shortwave and longwave radiation, wind speed, air temperature, air pressure, and specific humidity. Observed lake temperatures from 1 July through 31 August 2018 are for lake depths of 0, 1, 2, 3, 4, 5, 6, 7, 8, 10, 12, 14, and 16 m for model initialization and evaluation.

2.4 Experiment design

160 Simulations were conducted with both CLM-ORG and CLM-KPP from 1 July through 31 August 2018. The depth for this lake was set up to 20 m in both models. We divided the lake into 24 layers, with layer center point depths of 0.05, 0.15, 0.25, 0.35, 0.45, 1, 2, 3, 4, 5, 6, 7, 8, 9, 10, 11, 12, 13, 14, 15, 16, 17, 18, and 19.25 m. The lake temperatures were initialized with observations for 1 July. The WST and temperature profile simulations with CLM-ORG and CLM-KPP were compared with the observed lake
165 temperatures. The metrics used for evaluating the performance of the model included the root mean square error (RMSE) and correlation coefficient (R).

3 Results

3.1 Simulations with CLM-ORG and CLM-KPP

WST simulations with CLM-KPP were more accurate than those with CLM-ORG, especially in August.
170 The RMSE of WST decreased from 0.8 ˚C with CLM-ORG to 0.4 ˚C with CLM-KPP (Fig. 2). CLM-KPP also produced better vertical lake temperature profile simulations than CLM-ORG, particularly in mid to late August. The observations showed that the lake mixed on 16 August (Fig. 3a). CLM-KPP accurately captured the mixing event (Fig. 3c), while CLM-ORG estimated a stratified lake throughout the model period (Fig. 3b). Insignificant differences were seen between CLM-ORG and
175 CLM-KPP when compared to observations for the period before 16 August, while remarkable improvements were achieved with CLM-KPP during 16–31 August after the strong wind event

https://doi.org/10.5194/hess-2019-332
Preprint. Discussion started: 4 July 2019

Hydrology and Earth System Sciences
Discussions
Open Access
EGU

occurred (Figs. 3d-e). The RMSE of the temperature profile simulations decreased from 1.2 ˚C with CLM-ORG to 1.0 ˚C with CLM-KPP, and R increased from 0.90 to 0.95 (Table 1). In general, CLM-KPP had superior performance in simulating well-mixed conditions when compared with CLM-ORG, indicating a successful implementation of KPP into CLM.

Simulations of total eddy diffusivity (m^2/s) K_w^{KPP} with CLM-KPP were compared with those of K_w^{ORG} with CLM-ORG. K_w^{KPP} within the boundary layer was generally larger than K_w^{ORG}, especially in August (Fig. 4). Thermal forcing played a vital role in this enlarged diffusivity, which was considered only in CLM-KPP and not in CLM-ORG. However, the total eddy diffusivity with CLM-ORG was higher than that with CLM-KPP below the boundary layer (Fig. 4). The pattern of the diffusivity with CLM-ORG was consistent with that of the squared buoyancy frequency N^2 (Fig. 5), implying that the enhanced diffusivity (K_{ed}) was weighted very highly in K_w^{ORG} in this model. In the meantime, K_w^{KPP} was mostly on the order of 10^{-7} and was the product of internal-wave diffusivity, molecular diffusivity, and diffusivity due to shear instability (Eq. (9)). The first two terms were also on the order of 10^{-7}, indicating that the total eddy diffusivity with CLM-KPP was controlled mostly by these two terms. In early July, K_w^{KPP} sometimes appeared to be on the order of 10^{-5}, which was consistent with that of the last term, shear instability diffusivity, implying that this term dominated K_w^{KPP}. The diffusivity increase was closely related to the strong winds occurring at the same time (Fig. 4b).

The squared buoyancy frequency (N^2) of simulations with both CLM-KPP and CLM-ORG were also compared for our study period. N^2 was related to the water density gradient (Eq. (5)) determined by the temperature gradient in both models. A greater N^2 produced more stable water and stronger water stratification. From 1 July through 15 August, the simulated N^2 with CLM-KPP near the bottom of the boundary layer was slightly larger than that with CLM-ORG (Fig. 5). Thus, the simulated water stratification with CLM-KPP at the bottom of the boundary layer was stronger than that in CLM-ORG before 16 August. However, after 16 August, the maximum N^2 with CLM-ORG occurred in the middle layer of the lake, maintaining stratification there. Conversely, the maximum N^2 with CLM-KPP moved down to near the bottom of the lake during the same 16-day period (Fig. 5).

3.2 Analysis of CLM-KPP simulations

We examined our simulations and meteorological forcing data in detail to physically understand water

https://doi.org/10.5194/hess-2019-332
Preprint. Discussion started: 4 July 2019

Hydrology and Earth System Sciences
Discussions
Open Access
EGU

mixing conditions simulated by CLM-KPP, especially over the period of 16–31 August 2018. Figure 6a shows that downward shortwave radiation was 45 W m^{-2} less during 1–15 August (shaded area) than in July. Meanwhile, over the same period, air temperature and specific humidity decreased dramatically, while wind speed showed almost no trend (Figs. 6b-d). In this period, the simulated net radiation with CLM-KPP was 54 W m^{-2} lower than that for July (Fig. 6e). The turbulent heat flux, the sum of sensible and latent heat fluxes, increased over this 15-day period due mainly to the decreased air temperature and humidity (Fig. 6f). Figure 6g shows that buoyancy flux, defined as net radiation minus turbulent heat flux in the boundary layer with a different unit (m^2/s^3), was mostly negative during 1–15 August, showing that the lake was losing heat. Due to this heat loss, the temperature in the upper lake decreased, reducing the temperature difference between the upper and lower parts of the lake and thus weakening the stratification. Therefore, we can see that the boundary layer depth increased over the period of 1–15 August (Fig. 6h) when the wind had no systematic changes, but thermal forcing (buoyancy flux) played a significant role in this increase.

During 15–16 August, a wind event (12 m/s) mixed the lake, dramatically increasing the boundary layer depth in addition to the negative buoyancy flux. The deep boundary layer was maintained through the end of August, even though the winds returned to normal conditions. Such strong mixing was not seen in CLM-ORG, where the water stratification could not be broken up by the high wind event without help from thermal forcing. Hence, the negative thermal forcing had a critical effect on the strong mixing in our study lake, which was consistent with observations.

4 Conclusions

We improved lake mixing process simulations by applying the vertical mixing scheme KPP in CLM. The current vertical mixing scheme in CLM is driven mainly by winds, while KPP considers not only winds but surface thermal forcing as well. The improved lake model was applied to Fog 3 Lake in Arctic Alaska. Results indicate that the WST and lake temperature profile simulations using KPP are greatly improved when compared to the original vertical mixing scheme in CLM. During the transition season in August, the improvement is most obvious. This improvement is associated with negative heat flux and high wind, which can cause deepening of the boundary layer and strong mixing. However, the original vertical mixing scheme of CLM cannot capture these strong mixing events and causes a

https://doi.org/10.5194/hess-2019-332
Preprint. Discussion started: 4 July 2019

positive lake temperature bias in its simulation. The improved lake model should be useful for reliable lake process predictions and better ecosystem services.

https://doi.org/10.5194/hess-2019-332
Preprint. Discussion started: 4 July 2019

Hydrology and Earth System Sciences
Discussions
Open Access
EGU

Appendix

Lake temperature is calculated as follows:

$$\frac{\partial T}{\partial t} = \frac{\partial}{\partial z}\left\{K_w(z,t)\frac{\partial T}{\partial z}\right\} + \frac{1}{C_w}\frac{\partial \phi}{\partial z} \quad \text{(A1)}$$

where T is lake temperature (K) at depth z (m) and time t (s), ϕ is the absorbed solar radiation as a heat source term (W m^{-2}), C_w is the volumetric heat capacity of lake water (J m^{-3} K^{-1}), and K_w is the total eddy diffusivity (m^2 s^{-1}).

The non-dimensional flux profiles are calculated as follows:

$$\emptyset = \begin{cases} 1 + 5\zeta, & 0 \le \zeta \\ (1 - 16\zeta)^{-1/2}, & -1.0 \le \zeta < 0 \\ (-28.86 - 98.96\zeta)^{-1/3}, & \zeta < -1.0 \end{cases} \quad \text{(A2)}$$

The non-dimensional shape function $G(\sigma)$ is a third-order polynomial:

$$G(\sigma) = a0 + a1\sigma + a2\sigma^2 + a3\sigma^3 \quad \text{(A3)}$$

$a0$, $a1$, $a2$, and $a3$ are given as:

$$a0 = 0$$

$$a1 = 1$$

$$a2 = -2 + 3\frac{\upsilon(h)}{hw(1)} + \frac{\partial \upsilon(h)}{w(1)} + \frac{\upsilon(h)\partial w(1)}{hw(1)^2} \quad \text{(A4)}$$

$$a3 = 1 - 2\frac{\upsilon(h)}{hw(1)} - \frac{\partial \upsilon(h)}{w(1)} - \frac{\upsilon(h)\partial w(1)}{hw(1)^2}$$

where $\upsilon(h)$ is the water diffusivity as a function of lake depth (h), and $w(1)$ is the velocity scale at the bottom of the lake boundary layer.

$B(d)$ is the buoyancy difference calculated with a depth of d as:

$$g\left(1 - \frac{\rho_r}{\rho(d)}\right) \quad \text{(A5)}$$

V_t^2 is calculated as:

$$V_t^2(d) = \frac{C_v dN w_s(-\beta_T C_s \varepsilon)^{-1/2}}{Ri_c \kappa^2} \quad \text{(A6)}$$

where Ri_c = 0.25, C_v = 1.6, β_T = 0.2, and C_s = -98.96.

Code and data availability

The model configuration and the input data used in this study are available based on request.

https://doi.org/10.5194/hess-2019-332
Preprint. Discussion started: 4 July 2019

Author contribution

Qunhui Zhang conducted the modeling, performed the analysis, and drafted the manuscript; Jiming Jin designed the study, interpreted the results, and supervised the research; Xiaochun Wang contributed the original ideas of the research; Phaedra Budy and Nick Barrett provided observational data and helped the analysis; Sarah E. Null gave constructive comments on the results in this study. All the authors edited the manuscript.

Competing interests

The authors declare that they have no conflict of interest.

Acknowledgments

This work was supported by the National Natural Science Foundation of China [grant number 91637209] and a grant from the US National Science Foundation [grant number 1603088].

References

Arp, C. D., Jones, B. M., Liljedahl, A. K., Hinkel, K. M., and Welker, J. A.: Depth, ice thickness, and ice-out timing cause divergent hydrologic responses among Arctic lakes, Water Resour. Res., 51(12), 9379-9401, https://dx.doi.org/10.1002/2015WR017362, 2015.

Augusto-Silva, P. B., MacIntyre, S., de Moraes Rudorff, C., Cortés, A., and Melack, J. M.: Stratification and mixing in large floodplain lakes along the lower Amazon River, J. Great Lakes Res., 45(1), 61-72. https://dx.doi.org/10.1016/j.jglr.2018.11.001, 2019.

Banks, R. B.: Some features of wind action in shallow lakes, Proc. Am. Soc. Civ. Eng., 101, 813-827, 1975.

Berger, S. A., Diehl, S., Kunz. T. J., Albrecht, D., Oucible, A. M., and Ritzer, S.: Light supply, plankton biomass, and seston stoichiometry in a gradient of lake mixing depths, Limnol. Oceanogr., 51(4), 1898-1905, https://dx.doi.org/10.4319/lo.2006.51.4.1898, 2006.

Bonan, G. B.: Sensitivity of a GCM simulation to inclusion of inland water surface, J. Climate, 8(11), 2691-2704, https://dx.doi.org/10.1175/1520-0442(1995)008%3C2691:SOAGST%3E2.0.CO;2, 1995.

https://doi.org/10.5194/hess-2019-332
Preprint. Discussion started: 4 July 2019

Bryson, R. A., and Ragotzkie, R. A.: On internal waves in lakes, Limnol. Oceanogr., 5(4), 397-408, https://dx.doi.org/10.4319/lo.1960.5.4.0397, 1960.

Chiswell, S. M.: Annual cycles and spring blooms in phytolankton: Don't abandon Sverdrup completely, Mar. Ecol.-Prog. Ser., 443, 39-50, 2011.

Chowdhury, M. R., Wells, M. G., and Cossu, R.: Observations and environmental implications of variability in the vertical turbulent mixing in Lake Simcoe, J. Great Lakes Res., 41(4), 995-1009, https://dx.doi.org/10.1016/j.jglr.2015.07.008, 2015.

Dai, Y., Yao, T., Li, X., and Ping, F.: The impact of lake effects on the temporal and spatial distribution of precipitation in the Nam Co basin, Tibetan Plateau, Quatern. Int., 475, 63-69, https://dx.doi.org/10.1016/j.quaint.2016.01.075, 2018.

Diallo, I., Giorgi, F., and Stordal, F.: Influence of Lake Malawi on regional climate from a double-nested regional climate model experiment, Clim. Dynam., 50(9-10), https://dx.doi.org/10.1007/s00382-017-3811-x, 2017.

Dodson, S. I.: Introduction to limnology, J. N. Am. Benthol. Soc., 23(3), 661-662, https://dx.doi.org/10.1899/0887-3593(2004)023%3C0661:ITL%3E2.0.CO;2, 2004.

Ellis, C. R., Stefan, H. G., and Gu, R.: Water temperature dynamics and heat transfer beneath the ice cover of a lake, Limnol. Oceanogr., 36(2), 324-334, https://dx.doi.org/10.4319/lo.1991.36.2.0324, 1991.

Etemad-Shahidi, A., and Imberger, J.: Diapycnal mixing in the thermocline of lakes: Estimation by different methods, Environ, Fluid Mech., 6(3), 227-240, https://dx.doi.org/10.1007/s10652-005-4480-6, 2006.

Fang, X., and Stefan, H. G.: Long-term lake water temperature and ice cover simulations/measurements, Cold Reg. Sci. Technol., 24(3), 289-304, https://dx.doi.org/10.1016/0165-232X(95)00019-8, 1996.

Foley, B., Jones, I. D., Maberly, S. C., and Rippey, B., Long-term changes in oxygen depletion in a small temperate lake: Effects of climate change and eutrophication. Freshwater Biol., 57(2), 278-289, https://dx.doi.org/10.1111/j.1365-2427.2011.02662.x, 2012.

Goudsmit, G. H., Burchard, H., Peeters, F., and Wüest, A.: Application of k-ε turbulence models to enclosed basins: The role of internal seiches, J. Geophys. Res.- Oceans, 107(C12), 23-1-23-13, https://dx.doi.org/10.1029/2001JC000954, 2002.

https://doi.org/10.5194/hess-2019-332
Preprint. Discussion started: 4 July 2019

Gu, H., Jin, J., Wu, Y., Ek, M. B., and Subin, Z. M.: Calibration and validation of lake surface temperature simulations with the coupled WRF-lake model, Clim. Change, 129(3-4), 471-483, https://dx.doi.org/10.1007/s10584-013-0978-y, 2013.

Gu, H., Ma, Z., and Li, M.: Effect of a large and very shallow lake on local summer precipitation over the Lake Taihu basin in China, J. Geophys. Res.-Atmos., 121(15), 8832-8848, https://dx.doi.org/10.1002/2015JD024098, 2016.

Henderson-Sellers, B.: New formulation of eddy diffusion thermocline models, Appl. Math. Model., 9(6), 441-446, https://dx.doi.org/10.1016/0307-904X(85)90110-6, 1985.

Hostetler, S. W., and Bartlein, P. J.: Simulation of lake evaporation with application to modeling lake level variations of Harney-Malheur Lake, Oregon, Water Resour. Res., 26(10), 2603-2612, https://dx.doi.org/10.1029/WR026i010p02603, 1990.

Imberger, J.: The diurnal mixed layer, Limnol. Oceanogr., 30(4), 737-770, https://dx.doi.org/10.4319/lo.1985.30.4.0737, 1985.

Jan, H. G., and Verhagen.: Modeling phytoplankton patchiness under the influence of wind-driven currents in lakes, Limnol. Oceanogr., 39(7), 1551-1565, https://dx.doi.org/10.4319/lo.1994.39.7.1551, 1994.

Jeffries, M. O., Zhang, T., Frey, K., and Kozlenko, N.: Estimating late-winter heat flow to the atmoshere from the lake-dominated Alaskan north slope, J. Glaciol., 45(150), 315-324, https://dx.doi.org/10.3189/S0022143000001817, 1999.

Kheyrollah Pour, H., Duguay, C. R., Martynov, A., and Brown, L. C.: Simulation of surface temperature and ice cover of large northern lakes with 1-D models: A comparison with MODIS satellite data and in situ measurements, Tellus A, 64(1), 17614, https://dx.doi.org/10.3402/tellusa.v64i0.17614, 2012.

Krinner, G.: Impact of lakes and wetlands on boreal climate, J. Geophys. Res., 108(D16), 4520, https://dx.doi.org/10.1029/2002JD002597, 2003.

Kunze, E., Williams, A. J., and Briscoe, M. G.: Observations of shear and stability from a neutrally buoyant float, J. Geophys. Res., 95(C10), 18127-18142, https://dx.doi.org/10.1029/JC095iC10p18127, 1990.

https://doi.org/10.5194/hess-2019-332
Preprint. Discussion started: 4 July 2019

Laird, N. F., Desrochers, J., and Payer, M.: Climatology of lake-effect precipitation events over Lake Champlain, J. Appl. Meteorol. Clim., 48(2), 232-250, https://dx.doi.org/10.1175/2008JAMC1923.1, 2009.

Large, W. G., Mcwilliams, J. C., and Doney, S. C.: Oceanic vertical mixing: A review and a model with a nonlocal boundary layer parameterization, Rev. Geophys., 32(4), 363-403, https://dx.doi.org/10.1029/94RG01872, 1994.

Lewis, W. M.: The thermal regime of Lake Lanao (Philippines) and its theoretical implications for tropical lakes, Limnol. Oceanogr., 18(2), 200-217, https://dx.doi.org/10.4319/lo.1973.18.2.0200, 1973.

Li, X., Chao, Y., Mcwilliams, J. C., and Fu, L. L.: A comparison of two vertical-mixing schemes in a Pacific Ocean General Circulation Model, J. Climate, 14(7), 1377-1398, https://dx.doi.org/10.1175/1520-0442(2001)014%3C1377:ACOTVM%3E2.0.CO;2, 2001.

Liu, M., Zhang, Y., Shi, K., Zhu, G., Wu, Z., Liu, M., and Zhang, Y.: Thermal stratification dynamics in a large and deep subtropical reservoir revealed by high-frequency buoy data, Sci. Total Environ., 651, 614-624, https://dx.doi.org/10.1016/j.scitotenv.2018.09.215, 2019.

Lofgren, B. M.: A model for simulation of the climate and hydrology of the Great Lake basin, J. Geophys. Res., 109(D18), https://dx.doi.org/10.1029/2004JD004602, 2004.

Long, Z., Perrie, W., Gyakum, J., Caya, D., and Laprise, R.: Northern lake impacts on local seasonal climate, J. Hydrometeorol., 8(4), 881-896, https://dx.doi.org/10.1175/JHM591.1, 2007.

MacIntyre, S.: Describing fluxes within lakes using temperature arrays and surface meteorology, SIL Proceedings, 1922-2010, 30(3), 339-344, https://dx.doi.org/10.1080/03680770.2008.11902139, 2008.

MacIntyre, S., Fram, J. P., Kushner, P. J., Bettez, N. D., O'Brien, W. J., Hobbie, J. E., Kling, G. W., Williamson, C. E., Saros, J. E. G., and Vincent, W. F.: Climate-related variations in mixing dynamics in an Alaskan arctic lake, Limnol. Oceanogr., 54(6_part_2), 2401-2417, http://dx.doi.org/10.4319/lo.2009.54.6_part_2.2401, 2009.

Mahadevan, A., D'Asaro, E., Lee, C., and Perry, M. J.: Eddy-driven stratification initiates North Atlantic spring phytolankton blooms, Science, 337, 54-58, https://dx.doi.org/10.1126/science.1218740, 2012.

https://doi.org/10.5194/hess-2019-332
Preprint. Discussion started: 4 July 2019

Marshall, B. E., Ezekiel, C. N., Gichuki, J., Mkumbo, O. C., Sitoki, L., and Wanda, F.: Has climate change disrupted stratification patterns in Lake Victoria, East Africa? Afr. J. Aquat. Sci., 38(3), 249-253, https://dx.doi.org/10.2989/16085914.2013.810140, 2013.

Martynov, A., Sushame, L., and Laprise, R.: Simulations of temperate freezing lakes by one-dimensional lake models: Performance assessment for interactive coupling with regional cliamte models, Boreal Environ. Res., 15(2), 143-164, 2010.

Michalski, J., and Lemmin, U.: Dynamics of vertical mixing in the hypolimnion of a deep lake: Lake Geneva, Limnol. Oceanogr., 40(4), 809-816, https://dx.doi.org/10.4319/lo.1995.40.4.0809, 1995.

Mironov, D. V.: Parameterization of lakes in numerical weather prediction. Description of a lake model, COSMO Technology Report 11[R], Deutscher Wetterdienst, Offenbach am Main, Germany, 2008.

Monin, A. S., and Obukhov, A. M.: Basic laws of turbulent mixing in the atmospheric near the ground, Akad. Naud. SSSR Geofiz. Inst., 24(151), 163-187, 1954.

Oleson, K., Lawrence, D. M., Bonan, G. B., Drewniak, B., Huang, M., Koven, C. D., Levis, S., Li, F., Riley, W. J., Subin, Z. M., Swenson, S., Thornton, P. E., Bozbiyik, A., Fisher, R., Heald, C. L., Kluzek, E., Lamarque, J. F., Lawrence, P. J., Leung, L. R., Lipscomb, W., Muszala, S. P., Ricciuto, D. M., Sacks, W. J., Sun, Y., Tang, J., and Yang, Z.: Technical description of version 4.5 of the Community Land Model (CLM), NCAR Technical Note NCAR/TN-503CSTR, 420 pp., https://doi.org/10.5065/D6RR1W7M, 2013.

Patterson, J. C., Hamblin, P. F., and Imberger, J.: Classification and dynamic simulation of the vertical density structure of lakes, Limnol. Oceanogr., 29(4), 845-861, https://dx.doi.org/10.4319/lo.1984.29.4.0845, 1984.

Perroud, M., Goyette, S., Martynov, A., Beniston, M., and Anneville, O.: Simulation of multiannual thermal profiles in deep Lake Geneva: A comparison of one-dimensional lake models, Limnol. Oceanogr., 54(5), 1574–1594, https://dx.doi.org/10.4319/lo.2009.54.5.1574, 2009.

Peters, H., Gregg, M. C., and Sanford, T. B.: On the parameterization of equatorial turbulence: Effect of fine-scale variations below the range of the diurnal cycle, J. Geophys. Res., 100(C9), 18333-18348, https://dx.doi.org/10.1029/95JC01513, 1995.

Powell, T., and Jassby, A.: The estimation of vertical eddy diffusivities below the thermocline in lakes, Water Resour. Res., 10(2), 191-198, https://dx.doi.org/10.1029/WR010i002p00191, 1974.

https://doi.org/10.5194/hess-2019-332
Preprint. Discussion started: 4 July 2019

Roekel, L. P. V., Adcroft, A. J., Danabasoglu, G., Griffies, S. M., Kauffman, B., Large, W., Levy, M., Reichl, B., Ringler, T., and Schmidt, M.: The KPP boundary layer scheme: Revisiting its formulation and benchmarking one-dimensional ocean simulations relative to LES, J. Adv. Model. Earth Sy., 10(11), 2647-2685, https://dx.doi.org/10.1029/2018MS001336, 2018.

Rouse, W. R., Oswald, C. J., Binyamin, J., Spence, C., Schertzer, W. M., Blanken, P. D., Bussieres, N., and Duguay, C. R.: The role of northern lakes in a regional energy balance, J. Hydrometeorol., 6(3), 291-305, https://dx.doi.org/10.1175/JHM421.1, 2005.

Rouse, W. R., Blanken, P. D., Bussi ères, N., Walker, A. E., Oswald, C. J., Schertzer, W. M., and Spence, C.: An investigation of the thermal and energy balance regimes of Great Slave and Great Bear Lakes, J. Hydrometeorol., 9(6), 1318-1333, https://dx.doi.org/10.1175/2008JHM977.1, 2008,

Saber, A., James, D. E., and Hayes, D. F.: Effects of seasonal fluctuations of surface heat flux and wind stress on mixing and vertical diffusivity of water column in deep lakes, Adv. Water Resour., 119, 150-163, https://dx.doi.org/10.1016/j.advwatres.2018.07.006, 2018.

Samuelsson, P., Kourzeneve, E., and Mironov, D.: The impact of lakes on the European climate as simulated by a regional climate model, Boreal Environ. Res., 15(2), 113-129, 2010.

Shchepetkin, A. F., and Mcwilliams, J. C.: The regional oceanic modeling system (ROMS): A split-explicit, free-surface, topography-following-coordinate oceanic model, Ocean Model., 9(4), 347-404, https://dx.doi.org/10.1016/j.ocemod.2004.08.002, 2005.

Shimoda, Y., Azim, M. E., Perhar, G., Ramin, M., Kenney, M. A., Sadraddini, S., Gudimov, A., and Arhonditsis, G. B., Our current understanding of lake ecosytem response to climate change: What have we really learned from the north temperate deep lakes? J. Great Lakes Res., 37(1), 173-193, https://dx.doi.org/10.1016/j.jglr.2010.10.004, 2011.

Stanichny, S. V., Kubryakov, A. A., and Soloviev, D. M.: Parameterization of surface wind-driven currents in the Black Sea using drifters, wind, and altimetry data, Ocean Dynam., 66(1), 1-10, https://dx.doi.org/10.1007/s10236-015-0901-3, 2016.

Stepanenko, V., J öhnk, K. D., Machulskaya, E., Perroud, M., Subin, Z., Nordbo, A., Mammarella, I., and Mironov, D.: Simulation of surface energy fluxes and stratification of a small boreal lake by a set of one-dimensional models, Tellus A, 66(1), 21389, https://dx.doi.org/10.3402/tellusa.v66.21389, 2014.

https://doi.org/10.5194/hess-2019-332
Preprint. Discussion started: 4 July 2019

Stepanenko, V., Mammarella, I., Ojala, A., Miettinen, H., Lykosov, V., and Vesala, T.: LAKE 2.0: A model for temperature, methane, carbon dioxide and oxygen dynamics in lakes, Geosci. Model Dev., 9(5), 1977-2006, https://dx.doi.org/10.5194/gmd-9-1977-2016, 2016.

Stepanenko, V. M., Goyetter, S., Martynov, A., Perroud, M., Fang, X., and Mironov, D.: First steps of a Lake Model Intercomparison Project LakeMIP, Boreal Environ. Res., 15(2), 191-202, 2010.

Stepanenko, V. M., Martynov, A., Jöhnk, K. D., Subin, Z. M., Perroud, M., Fang, X., Beyrich, F., Mironov, D., and Goyette, S.: A one-dimensional model intercomparison study of thermal regime of a shallow turbid midlatitude lake, Geosci. Model Dev. Discuss., 5(4), 3993-4035, https://dx.doi.org/10.5194/gmdd-5-3993-2012, 2012.

Subin, Z. M., Riley, W. J., and Mironov, D.: An improved lake model for climate simulations: Model structure, evaluation, and sensitivity analyses in CESM1, J. Adv. Model. Earth Sy., 4, https://dx.doi.org/10.1029/2011MS000072, 2012.

Sun, X., Xie, L., Semazzi, F., and Liu, B.: Effect of lake surface temperature on the spatial distribution and intensity of the precipitation over the Lake Victoria basin, Mon. Weather Rev., 143(4), 1179-1192, https://dx.doi.org/10.1175/MWR-D-14-00049.1, 2015.

Sweers, H. E.: Vertical diffusivity coefficient in a thermocline, Limnol. Oceanogr., 15(2), 273-280, https://dx.doi.org/10.4319/lo.1970.15.2.0273, 1970.

Thiery, W., Davin, E. L., Panitz, H.-J., Demuzere, M., Lhermitte, S., and van Lipzig, N.: The impact of the African Great Lakes on the regional climate, J. Climate, 28(10), 4061-4085, https://dx.doi.org/10.1175/JCLI-D-14-00565.1, 2015.

Thorpe, S. A., and Jiang, R.: Estimating internal waves and diapycnal mixing from conventional mooring data in a lake, Limnol. Oceanogr., 43(5), 936-945, https://dx.doi.org/10.4319/lo.1998.43.5.0936, 1998.

Wang, X., Yi, C., Zhang, H., Farrara, J., Li, Z., Xin, J., Park, K., Colas, F., Mcwilliams, J. C., and Paternostro, C.: Modeling tides and their influence on the circulation in Prince William Sound, Alaska, Cont. Shelf Res., 63(4), S126-S137, https://dx.doi.org/10.1016/j.csr.2012.08.016, 2013.

Wu, J.: Wind-induced drift currents, J. Fluid Mech, 68(1), 49-70, https://dx.doi.org/10.1017/S0022112075000687, 1975.

https://doi.org/10.5194/hess-2019-332
Preprint. Discussion started: 4 July 2019

Hydrology and Earth System Sciences
Discussions
Open Access
EGU

Xu, L., Liu, H., Du, Q., and Lei, W.: Evaluation of the WRF-lake model over a highland freshwater lake in southwest China: Evaluation of the WRF-lake model, J. Geophys. Res.-Atmos., 121(23), 13,989-914,005, https://dx.doi.org/10.1002/2016JD025396, 2016.

Yang, P., Xing, Z., Fong, D. A., Monismith, S. G., Tan, K. M., and Lo, E. Y. M.: Observations of vertical eddy diffusivities in a shallow tropical reservoir, J. Hydro-environ. Res., 9(3), 441-451, https://dx.doi.org/10.1016/j.jher.2014.09.004, 2015.

Yao, H., Samal, N. R., Joehnk, K. D., Fang, X., Bruce, L. C., Pierson, D. C., Rusak, J. A., and James, A.: Comparing ice and temperature simulations by four dynamic lake models in Harp Lake: Past performance and future predictions, Hydrol. Processes, 28(16), 4587-4601, https://dx.doi.org/10.1002/hyp.10180, 2014.

Zhang, Q., Jin, J., Zhu, L., and Lu, S.: Modelling of water surface temperature of three lakes on the Tibetan Plateau using a physically based lake model, Atmos.-Ocean, 56(4), 289-295, https://dx.doi.org/10.1080/07055900.2018.1474085, 2018.

Zhu, L., Jin, J., Liu, X., Tian, L., and Zhang, Q.: Simulations of the impact of lakes on local and regional climate over the Tibetan Plateau, Atmos.-Ocean, 56(4), 230-239, https://dx.doi.org/10.1080/07055900.2017.1401524, 2017.

https://doi.org/10.5194/hess-2019-332
Preprint. Discussion started: 4 July 2019

Figures

Figure 1. Fog 3 Lake.

https://doi.org/10.5194/hess-2019-332
Preprint. Discussion started: 4 July 2019

Hydrology and Earth System Sciences
Discussions
Open Access
EGU

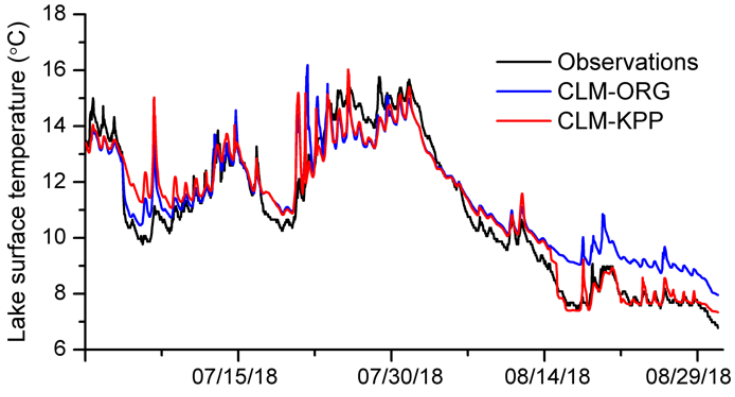

470

Figure 2. WST observations (black line) and simulations with CLM-ORG (blue line) and CLM-KPP (red line) (unit: ˚C).

https://doi.org/10.5194/hess-2019-332
Preprint. Discussion started: 4 July 2019

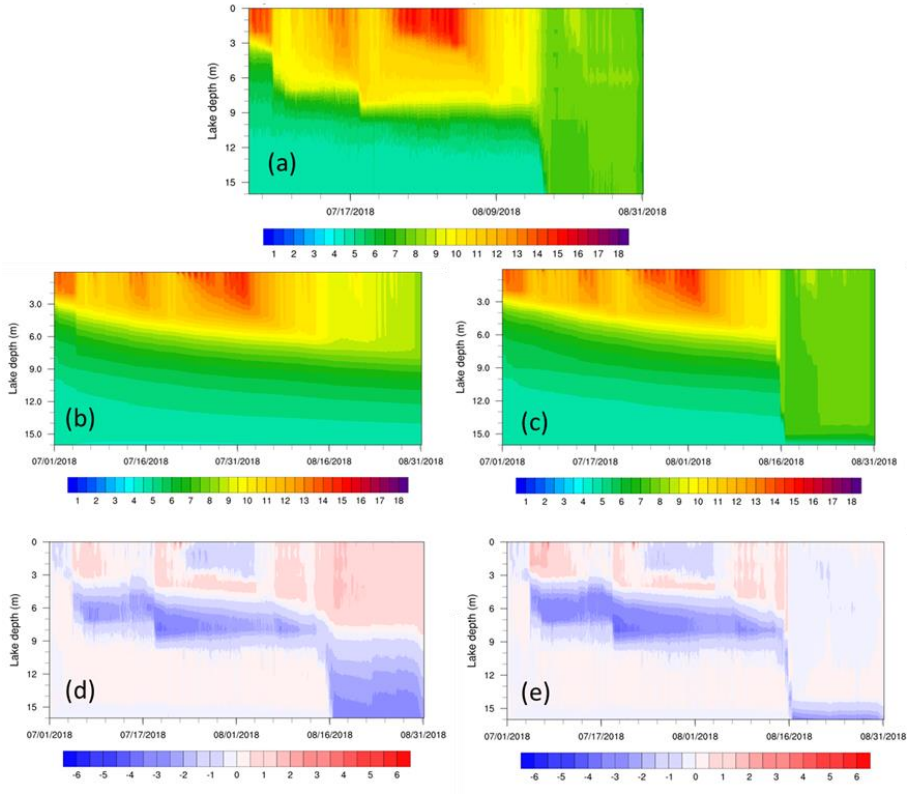

475 **Figure 3. Lake temperature profiles of (a) observations and simulations with (b) CLM-ORG and (c) CLM-KPP. Lake temperature profile differences between simulations and observations (d) CLM-ORG minus observations and (e) CLM-KPP minus observations (unit: ˚C).**

https://doi.org/10.5194/hess-2019-332
Preprint. Discussion started: 4 July 2019

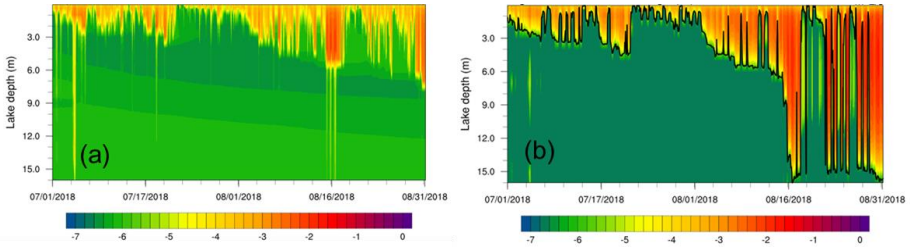

480

Figure 4. Simulated diffusivity for (a) CLM-ORG and (b) CLM-KPP on a logarithmic scale (Unit: m^2/s). The black line in (b) shows the lake boundary layer depth (Unit: m).

https://doi.org/10.5194/hess-2019-332
Preprint. Discussion started: 4 July 2019

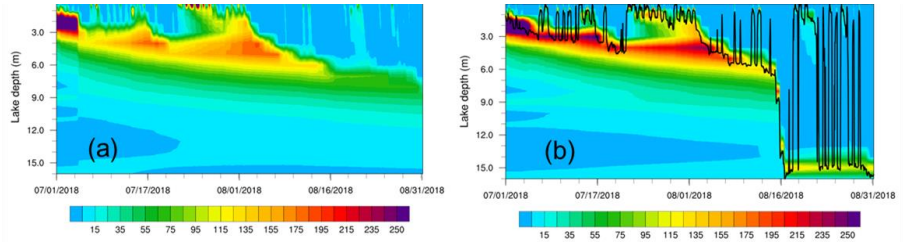

485

Figure 5. Simulated N^2 with (a) CLM-ORG and (b) CLM-KPP (Unit: $10^{-5}/s^2$). The black line in (b) shows the lake boundary layer depth (Unit: m).

https://doi.org/10.5194/hess-2019-332
Preprint. Discussion started: 4 July 2019

Hydrology and Earth System Sciences
Discussions
Open Access
EGU

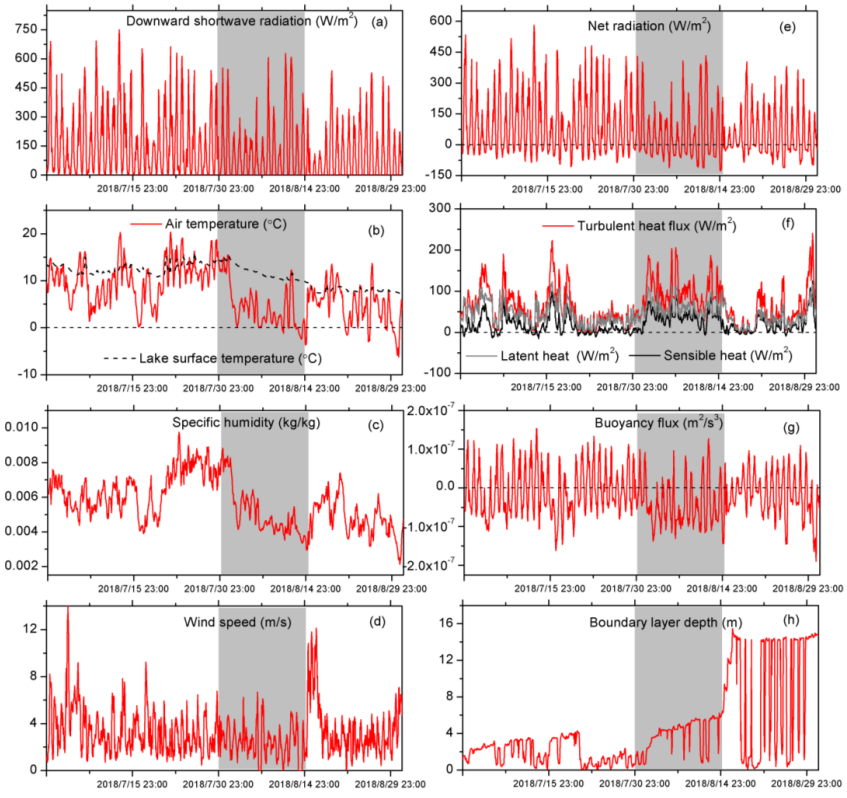

490 **Figure 6. Time series of (a) observed downward shortwave radiation (W/m^2), (b) observed air temperature and WST (°C), (c) observed specific humidity (kg/kg), (d) observed wind speed (m/s), (e) simulated net radiation (W/m^2), (f) simulated turbulent heat flux (W/m^2) (red line) with latent heat flux (gray line) and sensible heat flux (black line), (g) simulated buoyancy flux (m^2/s^3), and (h) simulated boundary layer depth (m). The gray shading covers 1 August through 15 August. The simulations were from CLM-KPP.**

https://doi.org/10.5194/hess-2019-332
Preprint. Discussion started: 4 July 2019

Hydrology and Earth System Sciences
Discussions
Open Access
EGU

495 **Table**

Table 1. RMSE (˚C) and R of the temperature profile simulations with CLM-ORG and CLM-KPP for the Alaskan lake.

	CLM-ORG	CLM-KPP
RMSE (˚C)	1.2	1.0
R	0.90	0.95